The Mid-Region of Parathyroid Hormone (1−34) Serves as a Functional Docking Domain in Receptor Activation†

Angela Wittelsberger,*,‡ Martina Corich,§ Beena E. Thomas,‡ Byung-Kwon Lee,§ Alessandra Barazza,§ Paul Czodrowski,|| Dale F. Mierke,|| Michael Chorev,⊥ and Michael Rosenblatt‡

Department of Physiology, Tufts University School of Medicine, 136 Harrison Avenue, Boston, Massachusetts 02111, and Departments of Chemistry and Molecular Pharmacology, Division of Biology and Medicine, Brown University, Providence, Rhode Island 02912

Received September 9, 2005; Revised Manuscript Received November 4, 2005

ABSTRACT: Elucidating the bimolecular interface between parathyroid hormone (PTH) and its cognate G protein-coupled receptor (PTHR1) should yield insights into the basis of molecular recognition and the mechanism of ligand-mediated intracellular signaling for a system that is critically important in regulating calcium levels in blood. We used photoaffinity scanning (PAS) to identify key ligand−receptor interactions for residues from the unstructured mid-region domain of PTH-(1−34). Four PTH analogues, containing a single photoreactive *p*-benzoylphenylalanine (Bpa) residue in position 11, 15, 18, or 21, were found to photo-cross-link within receptor regions [165−176], [183−189], [190−298], and [165−176], respectively. Addition of these mid-region contacts as constraints to our previously proposed model of the PTH−PTHR1 complex and extensive molecular simulation experiments enables substantial refinement of the model. Specifically, (1) the overall receptor-bound conformation of the hormone is not extended, but bent; (2) helix [169−176] of the N-terminal extracellular domain (N-ECD) of the receptor is redirected toward the heptahelical bundle; and (3) the hormone traverses between the top of transmembrane (TM) helices 1 and 2, rather than between TM-7 and TM-1. This significantly alters the model of both the receptor-bound tertiary structure of the hormone and the topological orientation of the C-terminus of the N-ECD in the hormone−receptor bimolecular complex. We propose that the mid-region of PTH-(1−34) has a role in fixing, by extensive contacts with the receptor, the entry of the N-terminal helix of the hormone into the heptahelical bundle between TM-1 and TM-2. This anchorage would orient the amino terminus into position to activate the receptor.

Parathyroid hormone (PTH)[1] regulates calcium levels in blood through its action on bone and kidney (*1*). These activities are mediated through interaction with its cognate receptor, PTHR1, a G protein-coupled seven transmembrane (TM) domain-containing receptor (GPCR) of Class II (Family B). Insights into the molecular basis of ligand recognition should advance understanding of the expression of PTH activity and aid the design of PTH-mimetics and antagonists for treatment of diseases such as osteoporosis, hypercalcemia of malignancy, and hyperparathyroidism (*2*).

Knowledge of structure−function relations and the three-dimensional structure of this receptor−ligand system comes from a variety of sources: chimeric receptors and hybrid ligands (*3*, *4*), deletion and site-directed mutants of the receptor (*5*, *6*), NMR of the ligand and distinct domains of the receptor (*7*−*9*), and photoaffinity scanning (PAS) of the hormone−receptor bimolecular interface (*10*−*16*). The PTH−PTHR1 interaction features strong binding between the C-terminus of PTH-(1−34) and the N-terminal extracellular domain (N-ECD) and sites in the first extracellular loop (ECL-1) of the receptor, while activation and signaling mainly results from interaction of the N-terminal half of PTH-(1−34) with sites on the extracellular part of the TM helices (*17*).

Integrating the structural information available, we recently proposed a model of the ligand−receptor bimolecular interface (*9*, *12*). In this model, the N-terminal half of PTH-(1−34) lies in a groove on top of the seven-TM bundle. The two first N-terminal residues of PTH-(1−34) reach toward the extracellular part of TM-5 and TM-6. The C-terminal

† This work was supported by Grants DK-47940 (to M.R.) and GM-54082 (to D.F.M.) from the National Institutes of Health, and postdoctoral fellowships from the Deutscher Akademischer Austauschdienst and the Suisse Fond National to A.W.

* To whom correspondence should be addressed: Angela Wittelsberger, Department of Physiology, Tufts University School of Medicine, 136 Harrison Ave., Boston, MA 02111. Phone, (617) 636-3882; fax, (617) 636-0445; e-mail, Angela.Wittelsberger@tufts.edu.

‡ Tufts University School of Medicine.

§ Participated when at Beth Israel Deaconess Medical Center/Harvard Medical School.

|| Brown University.

⊥ Current address: Harvard Medical School, Laboratory for Translational Research, 600 One Kendall Square, Cambridge, MA 02139.

[1] Abbreviations: PTH, parathyroid hormone; b, bovine; BNPS-skatole, 2-(2′-nitrophenylsulfenyl)-3-methyl-3-bromoindolenine; Bpa, *p*-benzoylphenylalanine; Bpa^n-PTH, [Bpa^n,Nle^{8,18},Arg^{13,26,27},L-2-Nal^{23},Tyr^{34}]bPTH(1-34)NH_2; CNBr, cyanogen bromide; ECL, extracellular loop; Endo-F, endoglycosidase F/*N*-glycosidase F; MD, molecular dynamics; Nal, naphthylalanine; N-ECD, N-terminal extracellular domain; Nle, norleucine; PBS, phosphate-buffered saline; RP-HPLC, reverse-phase high-performance liquid chromatography; SDS−PAGE, sodiumdodecyl sulfate−polyacrylamide gel electrophoresis; TM, transmembrane helix.

10.1021/bi051833a CCC: $33.50
Published on Web 01/27/2006

binding domain of PTH is extended away from the bundle, lying on the surface of the membrane, and interacting with residues in ECL-1 and the juxtamembrane portion of the N-ECD (*9*). Here, we present photo-cross-linking data on four new PTH-(1−34) analogues; each contains a photoreactive Bpa residue in the mid-region of the hormone, i.e., positions 11, 15, 18, and 21. Identification of the receptor contact sites for these analogues requires that the previously reported model of the hormone−receptor complex be reexamined.

EXPERIMENTAL PROCEDURES

Materials. Standard Boc-protected amino acid derivatives, *N*-hydroxybenzotriazole, *N*,*N*′-dicyclohexylcarbodiimide, and *p*-methylbenzhydrylamine resin were purchased from Applied Biosystems (Foster City, CA). Boc-Bpa-OH and Boc-Asp(OcHx)-OH were from Advanced ChemTech (Louisville, KY), and Boc-His(3-Bom)-OH was from Bachem (Bubendorf, Switzerland). Boc-Nle-OH was purchased from Chem-Impex International (Wood Dale, IL), dissolved in NMP to yield a 1 M solution, and loaded as such on the synthesizer. Boc-2′-Nal-OH was from Peptides International (Louisville, KY). Iodogen and 2-(2′-nitrophenylsulfenyl)-3-methyl-3-bromoindolenine (BNPS-skatole) were purchased from Pierce (Rockford, IL). CNBr was from Aldrich (Milwaukee, WI). $Na^{125}I$ was obtained from Amersham-Pharmacia (Arlington Heights, IL). Endo-F was obtained from New England BioLabs (Beverly, MA). ^3H-labeled adenine was from Perkin-Elmer Life Sciences (Boston, MA). All other chemical reagents were purchased from Aldrich/Sigma/Fluka Group (St. Louis, MO).

Peptide Synthesis. Bpa-containing analogues of [$Nle^{8,18}$, $Arg^{13,26,27}$,2′-Nal^{23},Tyr^{34}]PTH-(1−34)NH_2 were synthesized and purified as described previously (*18*). Purity of the peptides was confirmed by analytical RP-HPLC, and their structural integrity was determined by amino acid analysis and electrospray ionization mass spectrometry (ESI−MS). [Bpa^{11}]-PTH: MW, (calculated) 4321, (found) 4322; analytical RP-HPLC, t_R = 14.91 min (20−60% B, 30 min); peptide content, 72.6%. [Bpa^{15}]-PTH: MW, (calculated) 4321, (found) 4321; analytical RP-HPLC, t_R = 17.30 min (20−60% B, 30 min); peptide content, 66.1%. [Bpa^{18}]-PTH: MW, (calculated) 4321, (found) 4321; analytical RP-HPLC, t_R = 16.72 min (20−60% B, 30 min); peptide content, 57.7%. [Bpa^{21}]-PTH: MW, (calculated) 4335, (found) 4337; analytical RP-HPLC, t_R = 21.94 min (25−45% B, 30 min); peptide content, 69.9%.

Cell Culture. COS-7, HEK-293, and HEK293-C21 cells stably overexpressing recombinant hPTHR1 at ∼400 000 copies per cell were cultured as described (*19*).

Receptor Mutagenesis. Single-stranded phagemid DNA of PTHR1 was prepared by infecting the PTH1R-transformed *Escherichia coli* strain CJ236 with helper phage M13K07 (*20*). The [N176M]- and [V183M]PTHR1 site-directed mutants were constructed by oligonucleotide mutagenesis of the single-stranded phagemid DNA (*21*). Clones were selected, and the mutation was confirmed by DNA sequencing.

Transient Transfection of COS-7 Cells with Mutant Receptors. Six 15-cm dishes with COS-7 cells were transfected by addition of 5.2 μg/dish of DNA and 26 μL/dish of FuGENE 6 Transfection Reagent (Roche) in OPTI-MEM I Reduced Serum Medium (Gibco). The cells were harvested after 18 h for the photoaffinity cross-linking experiment.

Radioiodination and Photoaffinity Cross-Linking. Radioiodination of the Bpa-containing PTH analogues was carried out as previously described (*22*). Photoaffinity cross-linking and isolation of ligand−receptor conjugates was carried out as described (*14*, *16*).

PTHR1 Binding. Binding affinity of Bpa-containing analogues was determined using ^{125}I-[$Nle^{8,18}$,Tyr^{34}]-bPTH-(1−34)NH_2 as tracer (*18*). Assays were carried out using HEK-293-C2 cells. Receptor mutants were tested for binding affinity after transfection of COS-7 cells in 24 well-plates using 0.2 μg of DNA/well and 1 μL of FuGENE 6/well in OPTI-MEM.

Adenylyl Cyclase Activity. Activation of adenylyl cyclase by PTH analogues was determined in HEK293-C21 cells (*18*).

Luciferase Assay of Mutant Receptors. Transfection of COS-7 cells with either wild-type or mutant receptor was performed by adding 0.1 μg/well of mutant Rc DNA, 0.1 μg/well of CRE-luc, 0.1 μg/well of Renilla-luc, and 1 μL/well of FuGENE 6 to OPTI-MEM I. The assay was carried out after 18 h using the Dual-Glo Luciferase Assay System (Promega). Plates were read on a Mithras LB940 multilabel plate reader from Berthold Technologies.

Enzymatic and Chemical Digestions. Enzymatic digestions with Endo-F were carried out in 25 mM Tris-HCl, pH 8.5/0.01% SDS (w/v), at 37 °C for 2 h. BNPS-skatole digestions were carried out with 2 mg/mL freshly prepared BNPS-skatole in 70% acetic acid containing 0.1% SDS at 37 °C for 24−48 h in the dark. CNBr digestions were performed with 50 mg/mL freshly prepared CNBr in 70% formic acid containing 0.1% SDS at room temperature for 24 h in the dark. Glu-C digestions were carried out in acetate buffer, pH 4.3, for 4 h. Electrophoretic analyses were performed using 7.5% SDS−PAGE or 16.5% Tricine/SDS−PAGE. If needed, the radioactive bands were excised from the dried gels and extracted into 100 mM NH_4HCO_3, pH 7.5/0.01% SDS (w/v).

Molecular Modeling. The molecular model of the PTH receptor was built as described (*23*). The PTHR1 model was template-forced using the Discover molecular mechanics program and the X-ray structure of rhodopsin (*24*). The structural features of the fragment spanning the ectopic portion of TM-1 and the juxtamembrane portion of the N-ECD (PTHR1[168−198]), ECL-1 (PTHR1[241−285]), and ECL-3 (PTHR1[420−450])[2] were incorporated into the model using the experimentally determined distance restraints (*7*, *9*).

The model of the receptor was refined using the GROMACS program for the molecular dynamics (MD) simulations (*25*). A water/decane/water simulation cell (120 × 100 × 100 Å) was used to mimic the hydrophilic/hydrophobic, biphasic nature of the cytoplasmic membrane in a computationally simple model (*8*, *26*). During the simulations, the photoaffinity labeling-derived ligand−receptor interactions were maintained by distance restraints. A target distance of 14 Å between α-carbons of the Bpa residue in the ligand and the site of cross-linking in the receptor was chosen to

[2] Dale Mierke et al., unpublished results.

Table 1: Biological Evaluation of Binding Affinity and Adenylyl Cyclase Stimulatory Activity of Novel Bpa-Containing PTH Analogues[a]

PTH analogue	binding affinity IC_{50} (nM)	adenylyl cyclase activity EC_{50} (nM)
[Bpa[11]]-PTH	9.0 ± 2.5	7.0 ± 2.5
[Bpa[15]]-PTH	6.6 ± 1.4	1.1 ± 1.4
[Bpa[18]]-PTH	10.0 ± 2.6	22.0 ± 5.1
[Bpa[21]]-PTH	14.0 ± 3.2	2.2 ± 1.6
PTH	3.8 ± 0.5	1.0 ± 0.9

[a] The sequences are based on the [Nle[8],18, Arg[13,26,27],Nal[23],Tyr[34]]bPTH-(1−34)NH_2 scaffold. IC_{50} and EC_{50} values are expressed as mean values from three independent experiments. Assays were carried out using HEK293-C21 cells stably overexpressing hPTHR1 at 400 000 copies/cell (*19*).

provide ample freedom for the receptor and ligand to adjust and to optimize the ligand−receptor interactions. This distance accounts for the incorporation of Bpa in the photoaffinity labeling experiments, while the natural PTH ligand was used for the simulations.

RESULTS

Design and Synthesis of Bpa-Containing PTH Analogues. The four Bpa-containing PTH analogues were derived from the sequence [Nle[8,18],Arg[13,26,27],Nal[23],Tyr[34]]bPTH-(1−34)NH_2 (*16*) and are referred to hereafter as [Bpa[11]]-, [Bpa[15]]-, [Bpa[18]]-, and [Bpa[21]]-PTH. The purity of the analogues exceeded 97%, as assessed by analytical RP-HPLC; amino acid analysis and ESI−MS confirmed their structural integrity.

Biological Characterization. The novel Bpa-containing analogues showed binding affinities and adenylyl cyclase-stimulating activities similar to or slightly reduced compared to PTH-(1−34) (Table 1).

Photoaffinity Cross-Linking and Digestions. ^{125}I-[Bpa[11]]-PTH, ^{125}I-[Bpa[15]]-PTH, ^{125}I-[Bpa[18]]-PTH, and ^{125}I-[Bpa[21]]-PTH cross-linked to hPTHR1 expressed in stably transfected HEK293-C21 cells. Analysis by SDS−PAGE of the cross-linked photoconjugates showed a single diffuse band with an apparent relative molecular weight (M_r) of ∼87 kDa (data not shown), in agreement with previously reported M_r values for PTH−hPTHR1 photoconjugates (*14*). Photo-cross-linking to the parental HEK293 cells lacking the PTHR1 or to HEK293-C21 cells in the presence of excess (1 μM) of the nonradioactive parent PTH-(1−34) or the respective Bpa-containing PTH agonists did not yield the above-mentioned 87 kDa-band (data not shown). These results indicate that photo-cross-linking is PTHR1-specific and that the ligands bind competitively to the PTHR1. Treatment of the excised and eluted 87-kDa band with Endo-F shifted it to a narrow band of ∼60 kDa (not shown), representing the deglycosylated ^{125}I-[Bpa[xx]]PTH−PTHR1 photoconjugates. The purified ligand−receptor conjugates were analyzed by chemical and enzymatic digestions to determine the sites of receptor cross-linking.

PTHR1[165−298] Is a Common Conjugation Site for All Four PTH Analogues. Upon treatment of the ^{125}I-[Bpa[xx]]-PTH−PTHR1 photoconjugates with BNPS-skatole, an identical pattern of bands was obtained for all four analogues. Figure 1A shows a representative experiment with [Bpa[21]]-PTH. A band around 35 kDa (Figure 1A, lane 2) is obtained

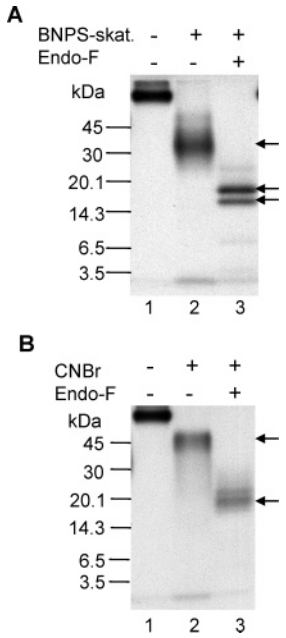

FIGURE 1: BNPS-skatole and CNBr digestions of the novel Bpa-containing PTH-(1−34) analogues. (A) Digestive pattern obtained after BNPS-skatole digestion of the ^{125}I-[Bpa[21]]-PTH−PTHR1 photoconjugate as a representative example. (B) Radiolabeled fragments obtained after CNBr digestion of the ^{125}I-[Bpa[21]]-PTH−PTHR1 photoconjugate as a representative example. The arrows indicate the product bands discussed in Results. Similar results were obtained in at least two additional experiments.

and shifts to 19 kDa when deglycosylated with Endo-F (lane 3). Clearly, the BNPS-skatole cleavage product contains glycosylation sites. The only fragment on the theoretical BNPS-skatole digestion map of PTHR1 consistent with this band is [165−298] (15.2 kDa, two glycosylation sites, Figure 2). Including the 4.3-kDa band contributed by the ligand, the 19-kDa band (lane 3, Figure 1A) therefore accounts for the deglycosylated product ^{125}I-[Bpa[21]]PTH−PTHR1[165−298]. The lower molecular weight band in lane 3 (Figure 1A) might be due to nonspecific cleavage at a cysteine or methionine residue, attributed to impurities in BNPS-skatole (*27*). We observed a similar two-band pattern for all four PTH analogues. From the BNPS-skatole digestions, we conclude that all four analogues cross-link within region [165−298] of the PTHR1.

PTHR1[165−189] Is a Common Conjugation Site for PTH Analogues Containing Bpa in Position 11, 15, or 21. Digestion of the [Bpa[11]]-, [Bpa[15]]-, and [Bpa[21]]-PTH−PTHR1 conjugates with CNBr resulted in a shift of the ∼87-kDa band of the intact conjugate to ∼50 kDa (Figure 1B, lanes 1 and 2). Isolation of the 50-kDa band and subsequent treatment with Endo-F generates a diffuse band at ∼19 kDa (Figure 1B, lane 3). Examining the theoretical CNBr digestion map of PTHR1 identifies PTHR1[64−189], containing all four glycosylation sites, as the region of cross-linking. Combined with the results obtained from the BNPS-skatole digestions, the overlapping sequence containing the cross-linking sites for [Bpa[11]]-, [Bpa[15]]-, and [Bpa[21]]-PTH is [165−189] located at the C-terminal portion of the N-ECD (Figure 2).

Position 15 in PTH-(1−34) Cross-Links within PTHR1-[183−189]. The contact site for position 15 was further refined by enzymatic digestion with endoproteinase Glu-C

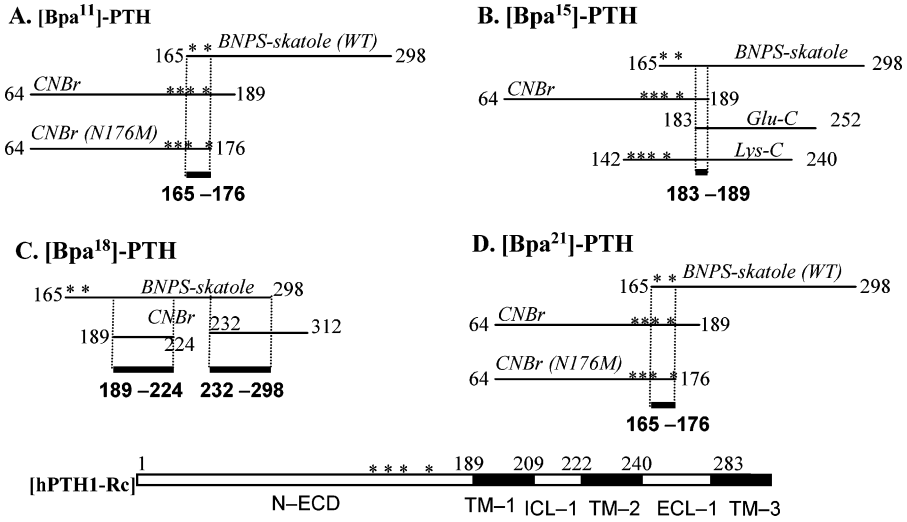

FIGURE 2: Schematics of the digestion pattern obtained from the different photoconjugates. The relevant receptor region is represented at the bottom. Fragments identified from BNPS-skatole, CNBr, Glu-C, and Lys-C digestions are shown for [Bpa[11]]- (A), [Bpa[15]]- (B), [Bpa[18]]- (C), and [Bpa[21]]-PTH (D). The superposing region containing the cross-linking site for each analogue is shown as a thick line. Glycosylation sites are marked with an asterisk.

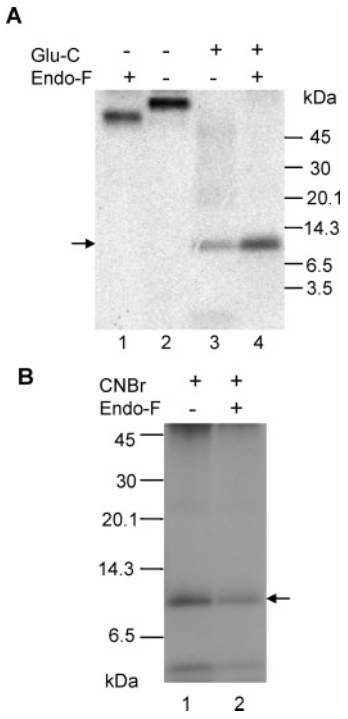

FIGURE 3: Glu-C digestion of ^{125}I-[Bpa[15]]-PTH−PTHR1 (A) and CNBr digestion of ^{125}I-[Bpa[18]]-PTH−PTHR1 (B). Arrows indicating the product bands are discussed in Results. Similar results were obtained in at least two additional experiments.

(Glu-C). The major band obtained upon cleavage of the glycosylated ^{125}I-[Bpa[15]]−PTHR1 conjugate with Glu-C is ~12 kDa (Figure 3A, lane 3). [Bpa[15]]-PTH contains glutamic acid residues in positions 4, 19, and 22. Cleavage at Glu[19] or Glu[22] separates the photo-cross-linking site (Bpa[15]) from the site carrying the ^{125}I tracer (Tyr[34]) in the ligand, releasing low molecular weight ligand fragments. When the exposure times to the enzyme were decreased and the digestion was carried out in acetate buffer at pH 4.3, ligand cleavage could be largely avoided (Figure 3A, lane 3). The ~12 kDa Glu-C-generated fragment could correspond to either [170−177] (13 kDa with ligand) or [183−252] (12.3 kDa with ligand) on the theoretical Glu-C cleavage map. These regions lie in or partially overlap the segment [165−189] deduced from CNBr and BNPS-skatole digestions. The region [170−177] contains one glycosylation site; [183−252] contains none. Consequently, treatment of the isolated 12-kDa band with Endo-F allows unambiguous identification. As shown in Figure 3A, lane 4, the Glu-C cleavage product is not glycosylated. Thus, the [183−252] receptor segment is the fragment obtained from Glu-C digestion (Figure 2B). Enzymatic digestion of the [Bpa[15]]-PTH−receptor conjugate with endoproteinase Lys-C identified receptor region [142−240] as containing the cross-linking site (Lys-C, Figure 2B, data not shown). Taken together, the contact site for position 15 lies within the CNBr/Glu-C-restricted heptapeptide sequence [183−189] of the N-ECD, close to the start of TM-1.

Position 18 in PTH-(1−34) Cross-Links within PTHR1-[190−224] or PTHR1[232−298]. For [Bpa[18]]-PTH, a ~9 kDa band was obtained after treatment of the intact 87 kDa ligand−receptor conjugate with CNBr (Figure 3B, lane 1). Isolation and digestion with Endo-F did not alter its electrophoretic mobility (lane 2), indicating that the fragment is not glycosylated. The theoretical CNBr digestion map of the PTHR1 contains two fragments that are both lacking in glycosylation sites and consistent in size with the observed band: PTHR1[190−224] at the top of TM-1 (8.3 kDa) and PTHR1[232−312] comprising the top of TM-2, ECL-1, and TM-3 (13.2 kDa). Together with the results from BNPS-skatole digestion, the site of cross-linking of position 18 must therefore lie within [190−298]. We tend to assign the CNBr-generated band to the conjugated fragment [190−224] that is closer in size to the observed ~9 kDa band. In the absence of further validation, we have not used the contact site of [Bpa[18]]-PTH as a restraint in the MD simulations.

Positions 11 and 21 in PTH-(1−34) Cross-Link within PTHR1[165−176]. For further refinement of the contact sites of positions 11 and 21 of PTH, we prepared receptor mutants [V183M]PTHR1 and [N176M]PTHR1, which contain an additional CNBr cleavage site within the [165−189] sequence. The mutant receptors showed binding affinities and cAMP/luciferase activities similar to wild-type receptor when

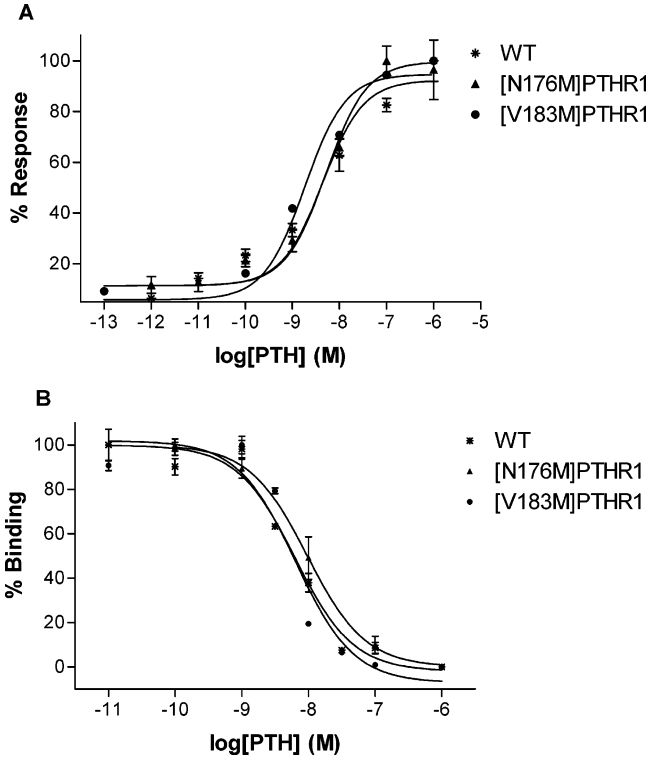

FIGURE 4: Biological characterization of mutant receptors [N176M]- and [V183M]PTHR1. Both assays were carried out with COS-7 cells transiently expressing the mutant or wild-type receptors. (A) Luciferase reporter assay; (B) competition binding assay.

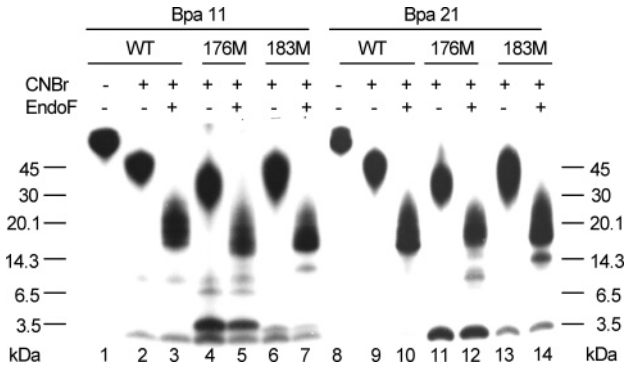

FIGURE 5: CNBr digestion of ^{125}I-[Bpa^{11}]-PTH (left panel) and ^{125}I-[Bpa^{21}]-PTH (right panel) conjugated to receptor mutants [N176M]-PTHR1 or [V183M]PTHR1. Similar results were obtained in at least two additional experiments.

transiently expressed in COS-7 cells (see Figure 4).

Theoretically, three radiolabeled fragments can be obtained by treatment of the ligand−[V183M]PTHR1 conjugates with CNBr. If cross-linking occurs to the methyl group of the Met-183 side chain, a low molecular weight band of 4.4 kDa corresponding to ligand−CH_3SCN should be obtained (*28*). Cross-linking to [64−183] should give rise to a 59-kDa band when glycosylated and to a 17.5-kDa band when deglycosylated. Cross-linking within [184−189] should yield a 5-kDa band both for the Endo-F-treated and nontreated sample. The experimentally obtained patterns are shown in Figure 5, lanes 6−7 and 13−14, for Bpa^{11}- and Bpa^{21}-PTH, respectively. A diffuse band similar in size to wild-type is obtained after CNBr digestion of the intact conjugates (lanes 6 and 13). The band shifts to ∼17 kDa when deglycosylated (lanes 7 and 14), identifying [64−183] as the receptor fragment obtained from CNBr digestion of both the [Bpa^{11}]- and the [Bpa^{21}]-PTH−[V183M]PTHR1 conjugates.

Treatment of the ligand−[N176M]PTHR1 conjugates with CNBr theoretically can generate three different receptor fragments: [176] (4.4 kDa), [64−176] (40.7 and 16.7 kDa when Endo-F-treated), or [177−189] (5.7 kDa, before and after Endo-F treatment). Experimentally, a band centered at ∼40 kDa is obtained after CNBr digestion of the intact conjugates (Figure 5, lanes 4 and 11) and shifts to ∼17 kDa when deglycosylated (lanes 5 and 12). This identifies receptor fragment [64−176] as the one observed. In addition, a 4.5-kDa band is seen in the case of [Bpa^{11}]-PTH (lanes 4 and 5). This could correspond to released ligand−CH_3SCN as a result of an additional cross-linking reaction to the methyl group of Met-176. It suggests that the cross-linking site of ^{125}I-[Bpa^{11}]-PTH may lie close to position [176] of the receptor. All results combined, the site of cross-linking for both ^{125}I-[Bpa^{11}]- and ^{125}I-[Bpa^{21}]-PTH lies within PTHR1-[165−176].

Molecular Modeling. The model obtained after MD simulations incorporating the newly identified contact sites as distant restraints shows significant changes compared to previous models of the PTH−PTHR1 complex (Figure 6). Most significantly, the ligand must adopt a loop structure in the mid-region in order to bring both Leu^{11} and Val^{21} in close proximity to PTHR1[165−176]. The N-terminal α-helix of PTH (residues 2−10) is maintained during the simulation; there is a slight translation (approximately 1 Å relative to the starting structure) of the N-terminal helix of PTH toward the N-ECD of the receptor. Despite this translation, the contacts between the N-terminus of the ligand (particularly Leu^5 and Met^8 of PTH) with the PTHR1 (*29*) are maintained in the revised model: both Leu^5 and Met^8 remain positioned within the hydrophobic core of the heptahelical bundle of the PTHR1 (*29*). Particularly important, the contact point between Ser^1 in PTH and Met-425 of the receptor, crucial for receptor activation, is maintained (*12*).

Another change involves the α-helical region [169−176] in the N-ECD of the PTHR1. During the MD simulations, this α-helix is found to fold underneath the C-terminal helix of the ligand. The driving force for this arrangement is a contact between this region of the receptor and residue 11 of PTH. These findings suggest a broad role for the N-ECD in determining ligand binding, involving interactions with not only the C-terminus of PTH, but also with the mid-region of the ligand.

During the MD simulations, an almost 90° bend of the two α-helices of PTH is observed. This arrangement is the result of simultaneous contacts between the hormone and both the proximal N-ECD of the PTHR1, described in this report, and Leu-261 in the center of ECL-1 (*14*).

DISCUSSION

Current understanding of the PTH/PTHR1 interaction has emphasized the critical roles of the N- and C-terminal helices of PTH-(1−34) in expression of hormonal bioactivity. The major contribution to hormone binding results from interactions of the C-terminal helix of PTH-(1−34) with the N-ECD of the receptor. The N-terminal helix of PTH-(1−34) is essential for receptor activation (*17*, *30*). In previous photoaffinity cross-linking studies, the first two N-terminal

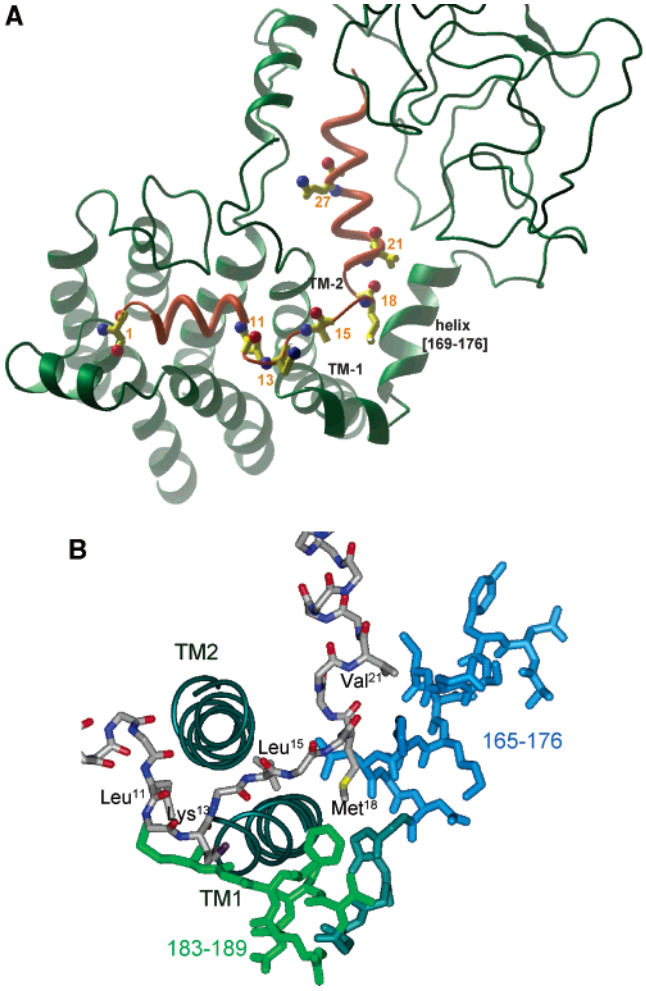

FIGURE 6: Model of the PTH-(1−34)−PTHR1 complex as obtained after MD simulations. (A) Extracellular view of the receptor (green) illustrating the interactions with the hormone (orange), including the N-terminal activation domain, the mid-region, and the C-terminal binding domain. Side-chains (yellow) are displayed for positions along the hormone sequence for which cross-linking sites were identified. The far N-terminus of the receptor, PTHR1[1−162], is shown for reference; no structural features are implied. (B) Expanded view of the PTH/PTHR1 complex, showing interactions within the mid-region of the hormone. TM-1 and TM-2 of the receptor are displayed as ribbons (dark green). The proximal N-terminus, PTHR1[165−189], is shown as sticks, with the identified cross-linking regions PTHR1[165−176] and PTHR1-[183−189] color-coded blue and green, respectively. The hormone is gray, with oxygen atoms in red and nitrogen atoms in blue.

residues of PTH were found to contact Met-425 in TM-6 of the PTHR1 (*12*). Photoaffinity labeling studies of the C-terminus of PTH-(1−34) indicate that all interactions of this region are located in the N-ECD or ECL-1 (*12*−*15*) of the receptor. Molecular models developed from these data describe interactions involved in ligand binding and receptor activation. However, the topological arrangement of the two functional domains in PTH-(1−34) and their interaction with receptor remain to be determined.

Using photoaffinity labeling, we targeted the mid-region of PTH, aiming to establish the arrangement between the N- and C-terminal domains when interacting with the receptor. The contact sites identified for [Bpa^{11}]-, [Bpa^{15}]-, and [Bpa^{21}]-PTH all lie within the membrane proximal region of the N-ECD. The only reported contact point here is between Arg-186 and position 13 of the ligand (*10*). In this study, [Bpa^{15}]-PTH cross-links within PTHR1[183−189], a domain that includes the cross-linking site for PTH position 13. [Bpa^{21}]-PTH cross-links within [165−176], farther away from TM-1 along the N-ECD. These contact points are accommodated by the previously proposed model of the ligand−receptor complex that consists of a ligand in extended conformation with the C-terminal helix of PTH projecting away from the seven-TM bundle, antiparallel to both the juxtamembrane portion of the N-ECD and the α-helix of ECL-1 (*9*, *29*).

Most importantly, [Bpa^{11}]-PTH cross-links to the same receptor region as [Bpa^{21}]-PTH, namely, [165−176]. This adds significant constraints to the conformational features of the ligand while bound. In the evolving model (Figure 6), the mid-region of the ligand must adopt a loop conformation.

The structure of PTH-(1−34) has been a point of contention for some time. A range of structures have been proposed, from an extended rod with 100% helix content (*31*), to a U-shaped tertiary structure with intramolecular helix−helix interactions (*32*), to an essentially nonstructured form (*8*). These conformations may be accessible to the ligand in different solvents (water, aqueous buffer, and water−trifluoroethanol mixtures), in the presence of micelles or in the crystalline state. One theory calls for the GPCR to adopt a number of conformational states, varying in activity (accounting for constitutive active receptors and inverse agonists), and proposes that ligand binding stabilizes the receptor in an active conformation. In such a model, ligands with slightly different conformations may bind and activate the receptor. Incorporating the new restraints for mid-region residues into the MD simulations results in a model in which the ligand, beginning at Leu^{11}, forms a rather large loop. This is the only way to accommodate the photoaffinity labeling results for [Bpa^{11}]- and [Bpa^{21}]-PTH.

In a similar fashion, we propose a change in receptor conformation. PTHR1[165−176] contains one of two amphipatic α-helices (i.e., [169−176] and [180−189]), located in the proximal end of the N-ECD, and suggested to lie on the surface of the membrane (*7*). Previous molecular modeling efforts positioned the two α-helices projecting away from the seven-TM bundle of the PTHR1. With the requirement of Leu^{11} to be in close proximity to PTHR1[165−176], the second helix [169−176] shifts toward the seven-TM bundle, moving slightly underneath the C-terminal helix of the ligand.

These conformational changes take place during the simulation to account for the new contact points. We have used very generous distance restraints of 14 Å for Cα−Cα during the simulations for each of these new contact points. This allows for complete freedom of the side chains of the ligand and receptor (the native sequence of PTH is used in the simulations) to adopt the most favorable conformation. The Bpa-containing ligands could conceivably capture the ligand/receptor complex at different stages of binding, and therefore, all contact points should not necessarily be applied simultaneously. However, on the basis of the transferred NOE results for PACAP (*33*), indicating very small conformational changes upon binding to this Class II GPCR, the large distance should certainly account for any conformational changes the ligand may undergo during the binding process.

The detailed interactions between the mid-region of PTH-(1−34) and residues in the juxtamembrane region of the N-ECD unambiguously define a key feature of the hormone−receptor complex: the N-terminus of PTH enters between the extracellular ends of TM-1 and TM-2 (versus the entry between TM-7 and TM-1, suggested in an earlier model (*34*)). The previous finding of [Bpa^{27}]-PTH cross-linking to Leu-261 also favors the TM-1/TM-2 entry (*9*). This role of the mid-region of PTH explains why PTH fragments shorter than 1−11 (i.e., lacking the entire mid-region) are unable to activate PTHR1 (*35*). In line with this, the interaction of the N-terminal portion of PTH-(1−34) with the external part of the TM bundle was found to be promoted by residues 15−20 of PTH (*36*).

The finding that [Bpa^{18}]-PTH cross-links to either [190−224] comprising the top of TM-1 or to [232−298], a large region that includes the top of TM-2, is consistent with the TM-1/TM-2 topological arrangement. From the model, binding interactions of position 18 of PTH can be with both the extracellular end of TM-1 (close to Met-189) and TM-2 (close to Lys-240) (see Figure 6). Indeed, position 19 of a PTHrP analogue was recently shown to cross-link to Lys-240 at the extracellular end of TM-2 of the receptor (*37*).

Our findings reveal that the N-ECD of the receptor is tightly involved in the binding of the ligand. This suggests a functional role for the mid-region of the hormone in guiding the N-terminal segment of the ligand into a binding groove in the heptahelical bundle. Therefore, we propose a three-step model for the ligand−receptor interaction. First, a binding interaction between residues in the C-terminal helix of the ligand and the N-ECD of the receptor dominates. Second, the mid-region of PTH-(1−34) forms contacts with the C-terminal part of the N-ECD, and a structural rearrangement takes place involving α-helix PTHR1[169−176]. In the third step, the N-terminal helix of the hormone reaches into the binding groove on the extracellular surface of the TM bundle, leading to receptor activation.

REFERENCES

1. Hock, J. M., Fitzpatrick, L. A., and Bilezikian, J. P. (2002) *Principles of Bone Biology* (Bilezikian, J. P., Raisz, L. G., and Rodan, G. A., Eds.) pp 463−481, Academic Press, San Diego, CA.
2. Chorev, M., and Rosenblatt, M. (2001) *The Parathyroids: Basic and Clinical Concepts* (Bilezikian, J. P., Marcus, R., and Levine, M., Eds.) pp 53−91, Academic Press, San Diego, CA.
3. Bergwitz, C., Gardella, T. J., Flannery, M. R., Potts, J. T., Jr., Kronenberg, H. M., Goldring, S. R., and Juppner, H. (1996) Full activation of chimeric receptors by hybrids between parathyroid hormone and calcitonin. Evidence for a common pattern of ligand−receptor interaction, *J. Biol. Chem. 271*, 26469−26472.
4. Juppner, H., Schipani, E., Bringhurst, F. R., McClure, I., Keutmann, H. T., Potts, J. T., Jr., Kronenberg, H. M., Abou-Samra, A. B., Segre, G. V., and Gardella, T. J. (1994) The extracellular amino-terminal region of the parathyroid hormone (PTH)/PTH-related peptide receptor determines the binding affinity for carboxyl-terminal fragments of PTH-(1-34), *Endocrinology 134*, 879−884.
5. Lee, C., Gardella, T. J., Abou-Samra, A. B., Nussbaum, S. R., Segre, G. V., Potts, J. T., Jr., Kronenberg, H. M., and Juppner, H. (1994) Role of the extracellular regions of the parathyroid hormone (PTH)/PTH-related peptide receptor in hormone binding, *Endocrinology 135*, 1488−1495.
6. Turner, P. R., Bambino, T., and Nissenson, R. A. (1996) A putative selectivity filter in the G-protein-coupled receptors for parathyroid hormone and secretion, *J. Biol. Chem. 271*, 9205−9208.
7. Pellegrini, M., Bisello, A., Rosenblatt, M., Chorev, M., and Mierke, D. F. (1998) Binding domain of human parathyroid hormone receptor: from conformation to function, *Biochemistry 37*, 12737−12743.
8. Pellegrini, M., Royo, M., Rosenblatt, M., Chorev, M., and Mierke, D. F. (1998) Addressing the tertiary structure of human parathyroid hormone-(1-34), *J. Biol. Chem. 273*, 10420−10427.
9. Piserchio, A., Bisello, A., Rosenblatt, M., Chorev, M., and Mierke, D. F. (2000) Characterization of parathyroid hormone/receptor interactions: structure of the first extracellular loop, *Biochemistry 39*, 8153−8160.
10. Adams, A. E., Bisello, A., Chorev, M., Rosenblatt, M., and Suva, L. J. (1998) Arginine 186 in the extracellular N-terminal region of the human parathyroid hormone 1 receptor is essential for contact with position 13 of the hormone, *Mol. Endocrinol. 12*, 1673−1683.
11. Behar, V., Bisello, A., Bitan, G., Rosenblatt, M., and Chorev, M. (2000) Photoaffinity cross-linking identifies differences in the interactions of an agonist and an antagonist with the parathyroid hormone/parathyroid hormone-related protein receptor, *J. Biol. Chem. 275*, 9−17.
12. Bisello, A., Adams, A. E., Mierke, D. F., Pellegrini, M., Rosenblatt, M., Suva, L. J., and Chorev, M. (1998) Parathyroid hormone-receptor interactions identified directly by photocross-linking and molecular modeling studies, *J. Biol. Chem. 273*, 22498−22505.
13. Gensure, R. C., Gardella, T. J., and Juppner, H. (2001) Multiple sites of contact between the carboxyl-terminal binding domain of PTHrP−(1- -36) analogs and the amino-terminal extracellular domain of the PTH/PTHrP receptor identified by photoaffinity cross-linking, *J. Biol. Chem. 276*, 28650−28658.
14. Greenberg, Z., Bisello, A., Mierke, D. F., Rosenblatt, M., and Chorev, M. (2000) Mapping the bimolecular interface of the parathyroid hormone (PTH)−PTH1 receptor complex: spatial proximity between Lys(27) (of the hormone principal binding domain) and leu(261) (of the first extracellular loop) of the human PTH1 receptor, *Biochemistry 39*, 8142−8152.
15. Mannstadt, M., Luck, M. D., Gardella, T. J., and Juppner, H. (1998) Evidence for a ligand interaction site at the amino-terminus of the parathyroid hormone (PTH)/PTH-related protein receptor from cross-linking and mutational studies, *J. Biol. Chem. 273*, 16890−16896.
16. Zhou, A. T., Bessalle, R., Bisello, A., Nakamoto, C., Rosenblatt, M., Suva, L. J., and Chorev, M. (1997) Direct mapping of an agonist-binding domain within the parathyroid hormone/parathyroid hormone-related protein receptor by photoaffinity crosslinking, *Proc. Natl. Acad. Sci. U.S.A. 94*, 3644−3649.
17. Vilardaga, J. P., Lin, I., and Nissenson, R. A. (2001) Analysis of parathyroid hormone (PTH)/secretin receptor chimeras differentiates the role of functional domains in the pth/pth-related peptide (PTHrP) receptor on hormone binding and receptor activation, *Mol. Endocrinol. 15*, 1186−1199.
18. Nakamoto, C., Behar, V., Chin, K. R., Adams, A. E., Suva, L. J., Rosenblatt, M., and Chorev, M. (1995) Probing the bimolecular interactions of parathyroid hormone with the human parathyroid hormone/parathyroid hormone-related protein receptor. 1. Design, synthesis and characterization of photoreactive benzophenone-containing analogs of parathyroid hormone, *Biochemistry 34*, 10546−10552.
19. Pines, M., Adams, A. E., Stueckle, S., Bessalle, R., Rashti-Behar, V., Chorev, M., Rosenblatt, M., and Suva, L. J. (1994) Generation and characterization of human kidney cell lines stably expressing recombinant human PTH/PTHrP receptor: lack of interaction with a C-terminal human PTH peptide, *Endocrinology 135*, 1713−1716.
20. Vieira, J., and Messing, J. (1987) Production of single-stranded plasmid DNA, *Methods Enzymol. 153*, 3−11.
21. Kunkel, T. A., Roberts, J. D., and Zakour, R. A. (1987) Rapid and efficient site-specific mutagenesis without phenotypic selection, *Methods Enzymol. 154*, 367−382.
22. Roubini, E., Duong, L. T., Gibbons, S. W., Leu, C. T., Caulfield, M. P., Chorev, M., and Rosenblatt, M. (1992) Synthesis of fully active biotinylated analogues of parathyroid hormone and parathyroid hormone-related protein as tools for the characterization of parathyroid hormone receptors, *Biochemistry 31*, 4026−4033.
23. Rolz, C., and Mierke, D. F. (2001) Characterization of the molecular motions of constitutively active G protein-coupled receptors for parathyroid hormone, *Biophys. Chem. 89*, 119−128.
24. Palczewski, K., Kumasaka, T., Hori, T., Behnke, C. A., Motoshima, H., Fox, B. A., Le Trong, I., Teller, D. C., Okada, T.,

Stenkamp, R. E., Yamamoto, M., and Miyano, M. (2000) Crystal structure of rhodopsin: a G protein-coupled receptor, *Science 289*, 739−745.

25. Berendson, H. J. C., van der Spoel, D., and van Drunen, R. (1995) GROMACS: a message-passing parallel molecular dynamics implementation, *Comput. Phys. Commun. 91*, 43−56.
26. Prado, G. N., Mierke, D. F., Pellegrini, M., Taylor, L., and Polgar, P. (1998) Motif mutation of bradykinin B2 receptor second intracellular loop and proximal C terminus is critical for signal transduction, internalization, and resensitization, *J. Biol. Chem. 273*, 33548−33555.
27. Henry, L. K., Khare, S., Son, C., Babu, V. V., Naider, F., and Becker, J. M. (2002) Identification of a contact region between the tridecapeptide α-factor mating pheromone of *Saccharomyces cerevisiae* and its G protein-coupled receptor by photoaffinity labeling, *Biochemistry 41*, 6128−6139.
28. Kage, R., Leeman, S. E., Krause, J. E., Costello, C. E., and Boyd, N. D. (1996) Identification of methionine as the site of covalent attachment of a *p*-benzoyl-phenylalanine-containing analogue of substance P on the substance P (NK-1) receptor, *J. Biol. Chem. 271*, 25797−25800.
29. Rolz, C., Pellegrini, M., and Mierke, D. F. (1999) Molecular characterization of the receptor−ligand complex for parathyroid hormone, *Biochemistry 38*, 6397−6405.
30. Carter, P. H., Juppner, H., and Gardella, T. J. (1999) Studies of the N-terminal region of a parathyroid hormone-related peptide (1-36) analog: receptor subtype-selective agonists, antagonists, and photochemical cross-linking agents, *Endocrinology 140*, 4972−4981.
31. Jin, L., Briggs, S. L., Chandrasekhar, S., Chirgadze, N. Y., Clawson, D. K., Schevitz, R. W., Smiley, D. L., Tashjian, A. H., and Zhang, F. (2000) Crystal structure of human parathyroid hormone 1-34 at 0.9-Å resolution, *J. Biol. Chem. 275*, 27238−27244.
32. Cohen, F. E., Strewler, G. J., Bradley, M. S., Carlquist, M., Nilsson, M., Ericsson, M., Ciardelli, T. L., and Nissenson, R. A. (1991) Analogues of parathyroid hormone modified at positions 3 and 6. Effects on receptor binding and activation of adenylyl cyclase in kidney and bone, *J. Biol. Chem. 266*, 1997−2004.
33. Inooka, H., Ohtaki, T., Kitahara, O., Ikegami, T., Endo, S., Kitada, C., Ogi, K., Onda, H., Fujino, M., and Shirakawa, M. (2001) Conformation of a peptide ligand bound to its G-protein coupled receptor, *Nat. Struct. Biol. 8*, 161−165.
34. Mierke, D. F., and Pellegrini, M. (1999) Parathyroid hormone and parathyroid hormone-related protein: model systems for the development of an osteoporosis therapy, *Curr. Pharm. Des. 5*, 21−36.
35. Shimizu, M., Potts, J. T., Jr., and Gardella, T. J. (2000) Minimization of parathyroid hormone. Novel amino-terminal parathyroid hormone fragments with enhanced potency in activating the type-1 parathyroid hormone receptor, *J. Biol. Chem. 275*, 21836−21843.
36. Shimizu, M., Shimizu, N., Tsang, J. C., Petroni, B. D., Khatri, A., Potts, J. T., and Gardella, T. J. (2002) Residue 19 of the parathyroid hormone (PTH) modulates ligand interaction with the juxtamembrane region of the PTH-1 receptor, *Biochemistry 41*, 13224−13233.
37. Gensure, R. C., Shimizu, N., Tsang, J., and Gardella, T. J. (2003) Identification of a contact site for residue 19 of parathyroid hormone (PTH) and PTH-related protein analogs in transmembrane domain two of the type 1 PTH receptor. *Mol. Endocrinol. 17*, 2647−2658.

BI051833A